This is a repository copy of *Phosphorus burial and diagenesis in the central Bering Sea (Bowers Ridge, IODP Site U1341): Perspectives on the marine P cycle*.

White Rose Research Online URL for this paper:
http://eprints.whiterose.ac.uk/80330/

Version: Submitted Version

Phosphorus burial and diagenesis in the central Bering Sea (Bowers Ridge, IODP Site U1341): Perspectives on the marine P cycle

C. März[1, 2], S.W. Poulton[3], T. Wagner[2], B. Schnetger[1], H.-J. Brumsack[1]

[1] School of Civil Engineering and Geosciences (CEGS), Newcastle University, Newcastle upon Tyne, NE1 7RU, UK (corr. author: christian.maerz@ncl.ac.uk)

[2] Institute for Chemistry and Biology of the Marine Environment (ICBM), Carl-von-Ossietzky University, 26129 Oldenburg, Germany

[3] School of Earth and Environment, University of Leeds, Leeds, LS2 9JT, UK

Abstract

To reconstruct the cycling of reactive phosphorus (P) in the Bering Sea, a P speciation record covering the last ~4 Ma was generated from sediments recovered during Integrated Ocean Drilling Program (IODP) Expedition 323 at Site U1341 (Bowers Ridge). A chemical extraction procedure distinguishing between different operationally defined P fractions provides new insight into reactive P input, burial and diagenetic transformations. Reactive P mass accumulation rates (MARs) are ~20-110 $\mu mol/cm^2/ka$, which is comparable to other open ocean locations but orders of magnitude lower than most upwelling settings. We find that authigenic carbonate fluorapatite (CFA) and opal-bound P are the dominant P fractions at Site U1341. An overall increasing contribution of CFA to total P with sediment depth is consistent with a gradual "sink switching" from more labile P fractions (fish remains, Fe oxides,

organic matter) to stable authigenic CFA. However, the positive correlation of CFA with Al content implies that a significant portion of the supposedly reactive CFA is non-reactive "detrital contamination" by eolian and/or riverine CFA. In contrast to CFA, opal-bound P has rarely been studied in marine sediments. We find for the first time that opal-bound P directly correlates with excess silica contents. This P fraction was apparently available to biosiliceous phytoplankton at the time of sediment deposition and is a long-term sink for reactive P in the ocean, despite the likelihood for diagenetic re-mobilisation of this P at depth (indicated by increasing ratios of excess silica to opal-bound P). Average reactive P MARs at Site U1341 increase by ~25% if opal-bound P is accounted for, but decrease by ~25% if 50% of the extracted CFA fraction (based on the lowest CFA value at Site U1341) is assumed to be detrital. Combining our results with literature data, we present a qualitative perspective of terrestrial CFA and opal-bound P deposition in the modern ocean. Riverine CFA input has mostly been reported from continental shelves and margins draining P-rich lithologies, while eolian CFA input is found across wide ocean regions underlying the Northern Hemispheric "dust belt". Opal-bound P burial is important in the Southern Ocean, North Pacific, and likely in upwelling areas. Shifts in detrital CFA and opal-bound P deposition across ocean basins likely occurred over time, responding to changing weathering patterns, sea level, and biogenic opal deposition.

1.1 Introduction

Phosphorus is a key biolimiting nutrient that exerts a major control on marine primary productivity over geological - and potentially shorter - time scales (Redfield, 1958; Codispoti, 1989; Krom et al., 1991; Van Cappellen and Ingall, 1996; Cotner et al., 1997; Tyrell, 1999; Benitez-Nelson, 2000; Filippelli, 2008). Marine productivity in the photic zone is, in turn, a key factor for the photosynthetic sequestration of the greenhouse gas CO_2 in the ocean interior and eventually in the sediments. Therefore, the amount of bioavailable P in the photic zone may directly influence the global carbon and nutrient cycles, and thus Earth's climate. In the upper layer of the oceans, P is taken up by phytoplankton that settles through the water column, is partially re-mineralized during sinking (Paytan et al., 2003), and eventually deposited at the sea floor (Froelich et al., 1982; Benitez-Nelson, 2000). In addition, P is delivered to the sea floor as hydroxyapatite fish remains (Suess, 1981; Posner et al., 1984; Schenau and de Lange, 2000, 2001; Matijevic et al., 2008), adsorbed to Fe (oxyhydr)oxides (Einsele, 1938; Berner, 1973; Slomp et al., 1996; Delaney, 1998; Poulton and Canfield, 2006), and as detrital P minerals (Faul et al., 2005; Paytan and Faul, 2007; Lyons et al., 2011). Phosphorus associated with opal frustules of marine algae is another, currently understudied, component of the oceanic P cycle where diatoms dominate primary productivity (e.g., North Pacific, Southern Ocean) (Latimer et al., 2006; Tallberg et al., 2008, 2009; Küster-Heins et al., 2010a; Lyons et al., 2011).

An important factor in the global P cycle is its burial into marine sediments, which regulates the oceanic reservoir of bioavailable P. Current calculations of the pre-anthropogenic oceanic P residence time range from 8,800 to 36,000 years, based on different estimates of reactive marine P sources, sinks, and reservoirs (e.g., Ruttenberg, 1993; Delaney, 1998; Benitez-Nelson, 2000; Ruttenberg, 2001; Baturin,

2003; Wallmann, 2003, 2010). In these calculations, the sink term (i.e., the burial

rate of reactive P into marine sediments) is a major uncertainty because reactive P

phases are affected by various biogeochemical transformations at and below the

sediment-water interface.

Under oxygen-depleted conditions, organic and Fe-bound P may be released into

the water column (Ingall et al., 1993; Ingall and Jahnke, 1997) due to the inhibition of

P uptake by microbes (Gächter et al., 1988;Jilbert et al., 2011; Steenbergh et al.,

2011) and the dissolution of Fe (oxyhydr)oxides (Sundby et al., 1992; Anschutz et al.,

1998; Virtasalo et al., 2005; Jordan et al., 2008).This can result in an overall

depletion of reactive P from the sediment under anoxic conditions (Filippelli, 2001;

Algeo and Ingall, 2007; März et al., 2008; Kraal et al., 2010). Post-depositional

processes ("sink switching") also affect reactive P burial on the long term by

transferring P between different particulate forms within the sediments (Ruttenberg

and Berner, 1993; Filippelli and Delaney, 1996; Delaney, 1998; Anderson et al.,

2001). Sink switching transforms P from labile phases (e.g., adsorbed/Fe-

bound/organic P) via an amorphous Ca-phosphate precursor (Van Cappellen and

Berner, 1991; Schenau et al., 2000; Gunnars et al., 2004) to diagenetically stable

authigenic carbonate fluorapatite (CFA). This process occurs in most marine

environments (Ruttenberg and Berner, 1993) and results in an increased reactive P

burial efficiency (Delaney, 1998; Wallmann, 2010).

In this study we evaluate P burial and diagenesis in Plio- to Pleistocene sediments of

the central Bering Sea. Applying a combination of quantitative geochemical analyses

and a sequential P extraction, we show how depositional and diagenetic processes

affected the fractionation of P and reactive P mass accumulation rates in the Bering

Sea. Based on available data, we estimate how the recognition and interpretation of

certain sedimentary P fractions can have wider implications for the reconstruction of the P cycle in ocean regions comparable to the Bering Sea (i.e., high biosilica productivity, high eolian/riverine input).

1.2 Material and Methods

Sample material was obtained in 2009 during IODP Expedition 323 to the Bering Sea (Expedition 323 Scientists, 2010; Takahashi et al., 2011) from Site U1341 (western flank of Bowers Ridge; 54° 02.00' N, 179° 00.52' E; ~2140 m water depth) (Fig. 1). Sediment cores were retrieved from the United States Implementation Organization (USIO) drill ship JOIDES Resolution by the Advanced Piston Coring (APC, to 458 m drilling depth below sea floor, DSF) and the Extended Coring Barrel (XCB, to 600 m DSF) systems. The composite record was established as a splice of Holes 1341A, B and C. The age model is based on shipboard magneto- and biostratigraphy (Expedition 323 Scientists, 2010; Takahashi et al., 2011), and revised datums obtained by onshore biostratigraphic studies (Onodera et al., 2013). Extrapolating linear sedimentation rates beyond the oldest datum (~3.87 Ma) results in a maximum sediment age of ~4.3 Ma at Site U1341 (Takahashi et al., 2011).

Sediments at Site U1341 dominantly consist of biogenic opal and detrital clay to silt, with minor sand layers, volcanic ash beds, semi-lithified authigenic carbonate layers and biogenic carbonate (Aiello and Ravelo, 2012). Shipboard geochemical analyses involved pore water extraction by pressure squeezing of whole rounds and subsequent determination of iron, phosphate and alkalinity, as well as total organic carbon (TOC) analysis. Respective methods and data are published in the IODP Expedition 323 Preliminary Report and Proceedings (Expedition 323 Scientists, 2010;

Takahashi et al., 2011). For further geochemical analyses, ~190 sediment samples were obtained onboard from whole-round pore water squeeze cake residues (~10 cm thickness) and discrete plastic scoop samples (2 cm thickness), and stored frozen until further processing. Onshore, sediment samples were freeze-dried and ground in an agate ball mill. Instantaneous freezing after onboard sampling followed by rapid onshore freeze-drying guaranteed minimum air exposure, preventing oxidation of pyrite and possible effects on P speciation in these samples (Lukkari et al., 2007; Kraal et al., 2009).

Around 700 mg of each sample were mixed with 4200 mg of dilithiumtetraborate ($Li_2B_4O_7$, Spectromelt A10), pre-oxidized at 500°C with ~1000 mg NH_4NO_3, and fused to homogeneous glass beads. Glass beads were analysed for Al, Si and P contents by wavelength-dispersive X-ray fluorescence (XRF, Philipps PW 2400). Analytical precision and accuracy were better than 5%, as checked by in-house and international standard materials. The Si and P data are displayed as excess element contents relative to Upper Continental Crust (UCC; Wedepohl, 1995) to illustrate element enrichments or depletions relative to the background sediment composition ($element_{xs} = element_{sample} - Al_{sample} * (element/Al)_{UCC}$) (Brumsack, 2006). Mass accumulation rates (MAR, $\mu mol/cm^2/ka$) were calculated by multiplying dry bulk densities from onboard moisture and density (MAD) measurements [g/cm^3] (Expedition 323 Scientists, 2010; Takahashi, Ravelo, Alvarez Zarikian et al., 2011) with the respective P fraction [μmol] and linear sedimentation rates [cm/ka].

To constrain the phase associations of P in Bering Sea sediments, a sequential extraction scheme adapted from Ruttenberg (1992), Schenau and De Lange (2000), and Latimer et al. (2006) was applied to ~100 freeze-dried sediment samples (Table 1). The extractions yield six operationally defined P fractions that are leached with

specific extraction reagents. The frequently applied and well-tested SEDEX scheme (Ruttenberg, 1992; Ruttenberg et al., 2009) differentiates between loosely adsorbed P, P bound to Fe (oxyhydr)oxides, authigenic apatite, detrital apatite, and organic P (here referred to as extraction steps 1-5, respectively). Step 1 was modified by Schenau and De Lange (2000) to determine P bound to fish remains and/or amorphous Ca-phosphates. Latimer et al. (2006) added an extraction step for opal-associated P (Step 6). According to Ruttenberg (1992), reactive P is defined as the sum of all sequentially extracted P fractions without detrital apatite (Step 4).

The P extracted during steps 1, 3, 4 and 5 was analysed by the molybdate blue method using a UV/Vis spectrophotometer (Thermo Genesys 6, 880 nm) (Strickland and Parsons, 1972). The P extracted during steps 2 and 6 was analysed by Inductively Coupled Plasma Optical Emission Spectrometry (ICP-OES, Varian Vista-MPX). This technique was preferred for step 6 because the photometric quantification of opal-bound P described by Latimer et al. (2006) failed due to the strong interference of the molybdate colour complexes formed with both phosphate and silicic acid (Henriksen, 1966; Campbell and Thomas, 1970; Neal et al., 2000). As the studied sediments contain much more opal-bound Si than opal-bound P, this P fraction is overestimated by photometric analyses. A photometric interference has also been reported for the citrate-containing extraction solution used during step 2 (Lanzetta et al., 1979; Ruttenberg, 1992), and thus ICP-OES was used to determine P in this extract. Parallel ICP-OES analysis of opal-bound P and Si failed due to Si concentrations in the extraction solutions exceeding those of P by several orders of magnitude.

Triplicate extractions and analyses were performed on three samples from the top, middle and bottom of the U1341 record to test the reproducibility of the extraction

technique. The resulting relative standard deviations (RSD) range from 1 to 13%, depending on the relative contents of the respective P fractions (Table 1). Thus, despite the operationally-defined nature of the sequential extraction scheme (Ruttenberg, 1992), our data are internally consistent. All data are provided as Supplementary Information.

1.3 Results

1.3.1 Bulk element analysis

As shown in a study on the general geochemistry of Pliocene-Pleistocene Bowers Ridge deposits (März et al., 2013), Al_2O_3 and SiO_2 are the main constituents of the sediments at Site U1341 (Fig. 2). At 60-80 wt%, SiO_2 is clearly dominant (Fig. 2), but with an overall decrease from older to younger sediments. The Al_2O_3 record (2-15 wt%) shows an opposing overall trend, with values that increase upcore (Fig. 2). Mutual dilution of SiO_2 and Al_2O_3 is illustrated by a negative linear correlation coefficient (R^2) of 0.86 (März et al., 2013). While the Al_2O_3 record documents the input of fine-grained terrigenous siliciclastic material (e.g., clay minerals, feldspars), the SiO_2 record is mostly shaped by the variable contents of biogenic opal at Site U1341 (Aiello and Ravelo, 2012; März et al., 2013). The Si_{xs} record (i.e., the fraction of Si in excess of UCC) shows consistently positive values, implying that sediments at Site U1341 are enriched in Si relative to UCC over the last ~4.3 Ma as a result of biogenic opal deposition (März et al., 2013; Onodera et al., 2013). The intervals between 210 and 380 m CCSF-B and below 500 m CCSF-B are the most Si-enriched, with several Si_{xs} peaks between 20 and 35 % (Fig. 2). Total P contents vary from 100 to 624 ppm (average of 305 ppm; UCC = 757 ppm; Wedepohl, 1995)

with a slight overall trend towards higher P contents in younger sediments. Calculating P_{xs} contents (analogous to Si_{xs}) results in negative values throughout most of the record, implying that in contrast to Si, the sediments are slightly depleted in P relative to UCC (Fig. 2). The shipboard TOC record shows an overall increase towards younger sediments, with values mostly between 0.2 and 1.0 wt% (Fig. 2).

1.3.2 Sequential P extraction

The absolute P contents and relative contributions of each of the six sequential extraction steps to total P are displayed against sediment depth in Figures 3 and 4, respectively. Average contributions of the different P fractions to total P, as well as the relative percentage of reactive P (with/without opal-bound P and detrital CFA) against sediment depth are shown in Figure 5. Figure 6a displays reactive P MARs (with/without opal-bound P and detrital CFA). Collectively, these figures document the contributions of the extracted P fractions over the Site U1341 record.

Both Fe-bound P (Step 2) and organic P (Step 5) are of minor importance, with average contents of 7 and 19 ppm, respectively (corresponding to 2 and 6% of total P; Fig. 5a). The contribution from fish remains (Step 1) is also low over most of the record (on average 28 ppm and 10% of total P; Fig. 5a) apart from isolated peaks where fish remains reach up to 44% of total P, and these are also recognised in the bulk P record (Fig. 4). The overall shape of the detrital apatite record (Step 4) is similar to the fish remains, with mostly low values (on average 47 ppm and 16% of total P; Fig. 5a) and some isolated maxima reaching up to 55% of total P (Fig. 4).

The overall dominant P fractions at Site U1341 are authigenic CFA (Step 3) and opal-bound P (Step 6). Authigenic CFA contributes on average 105 ppm and 35% to

total P (Fig. 5a), with a clear trend to higher values below ~100 m CCSF-B (up to 180 ppm and 47% of total P; Figs. 3, 4). Opal-bound P averages 49 ppm and 17% of total P (Fig. 5a), but shows highest contents in the middle part of the record (maxima of 100 ppm and 39% of total P; Figs. 3, 4). Taken together, the contribution of reactive P in the studied sediments (including opal-bound P) is on average 208 ppm and 70% of total P, showing a dominance of reactive over non-reactive (i.e., detrital mineral-bound) P at Site U1341 (Fig. 5b). Without the contribution of opal-bound P, the reactive P contribution would be reduced to an average of 53% (Fig. 5b). The resulting reactive P MARs at Site U1341 are 23-107 $\mu mol/cm^2/ka$ (including opal-bound P) and 17-89 $\mu mol/cm^2/ka$ (excluding opal-bound P), with average MARs of 57.5 and 43.9 $\mu mol/cm^2/ka$, respectively (Fig. 6a).

Regarding relationships between the extracted P fractions and the bulk composition of the sediment, the authigenic CFA fraction correlates positively with Al contents (R^2 = 0.76), and negatively with Si_{xs} contents (R^2 = 0.75; Fig. 7). In contrast, the opal-bound P fraction is most important in the most Si-enriched samples (Figs. 2, 4), and there is a moderate yet significant positive correlation between opal-bound P and Si_{xs} (R^2_{linear} = 0.53; $R^2_{logarithmic}$ = 0.59; Fig. 7). The average weight (molar) ratio between Si_{xs} (i.e., opal-bound Si) and opal-bound P is ~4,290 (~4,730), with a trend to increasing Si_{xs}/opal-bound P ratios downcore (Fig. 6b), and a clear positive correlation between Si_{xs}/opal-bound P ratios and Si_{xs} contents (Fig. 7). The residual P correlates positively with Al, but with a slightly lower correlation coefficient (R^2 = 0.65) than the CFA fraction (Fig. 7). The remaining P fractions show no relationships with bulk geochemical parameters.

Comparing the sum of all extracted P fractions to the total P contents as determined by XRF (Figs. 3 a, b), the sequential extraction steps recovered on average ~85% of

total sedimentary P. While the nature of the residual P pool is unknown, earlier studies (Ruttenberg, 1992; Lukkari et al., 2007a; Küster-Heins et al., 2010b) also found that the SEDEX procedure did not extract all sedimentary P. The physical loss of sample during the SEDEX procedure (i.e., by decanting the supernatant extraction solution) might account for this incomplete recovery (Ruttenberg, 1992). However, comparison with an updated version of the extraction scheme (SPExMan-SEDEX; Ruttenberg et al., 2009) showed that a careful application of the "classical" SEDEX protocol should not result in significant sample loss. Consequently, another explanation for the residual P fraction at Site U1341 appears likely, particularly given the clear positive correlation between the P recovery and the Al contents of the samples (Fig. 7), such that the P extraction recovery was lowest in Al-rich samples, and highest in Si-rich samples (Fig. 4).

4.1 Discussion

At IODP Site U1341, the combination of sequential P extraction and total element analyses provides insights into the reactive and non-reactive P pools in the Plio-Pleistocene Bering Sea sediments. Despite the obvious spatial limitation of our data-set, the findings related to the CFA and opal-associated P fractions are transferrable to other, comparable parts of the world ocean, and question some conceptions of the global oceanic P cycle. Figure 8 illustrates P sources, transfer processes, and sinks in the Bering Sea water column (photic zone, intermediate to deep waters) and sediments (above and below ~50 m depth). Here, we discuss the different P fractions at Site U1341 regarding reactive and non-reactive P pools, and related paleoenvironmental conditions and processes.

4.1.1 Detrital input and the non-reactive P contribution

The non-reactive fraction of sedimentary P, defined as mineral-bound P that was not bioavailable prior to its deposition at the sea floor and does not undergo phase changes upon burial (Fig. 8), comprises P in well-crystallised detrital heavy minerals (e.g., magmatic/metamorphic fluorapatite; Ruttenberg, 1992). Zhang et al. (2010) reported detrital P as the dominant P pool in surface sediments of the shallow Bering Sea shelf, mostly delivered by the Yukon River (Dornblaser and Striegl, 2007) draining magmatic and metamorphic rocks. However, the delivery of riverine detrital P to an open marine setting like Bowers Ridge requires efficient offshore transport by strong currents, winds, and/or sea ice. This additional transport step probably explains the overall minor contribution of detrital P at Site U1341 (Fig. 5a).

At Site U1341, the positive correlation between the non-extractable P record (in % of total P) and the Al record (Fig. 7) indicates that the residual P pool is bound to terrigenous sediments. Possible explanations for this relationship include incomplete extraction of a) detrital apatite or other highly refractory P minerals (e.g., xenotime, monazite) during Step 4, b) P bound to highly refractory non-extractable organic material (Ruttenberg and Goni, 1997), or c) clay-bound P for which the SEDEX method was not calibrated (Walker and Syers, 1976; Ruttenberg, 1992). All these explanations suggest that the non-extractable P fraction was derived from a terrestrial source and can be defined as non-reactive P, similar to the operationally defined detrital P fraction (Fig. 8).

4.1.2 Redox and diagenetic effects on fish remains, organic P, and Fe-bound P

The quantitatively less important P phases extracted at Site U1341 are fish remains, Fe-bound P, and organic P (Figs. 3, 4). However, this merely reflects the low preservation potential of these P phases in the sediments, and not their probably much larger contribution to the transfer of P from the surface waters to the sea floor (Fig. 8) (Froelich et al., 1988; Slomp et al., 1996; Küster-Heins et al., 2010a, b). Numerous studies have shown that bottom water oxygen contents below ~20 µM (Wallmann, 2010) may lead to the recycling of Fe-bound and organic P from the sediment to the bottom waters (Ingall et al., 1993; Algeo and Ingall, 2007; Mort et al., 2010; Jilbert et al., 2011). The southern Bering Sea exhibits an oxygen minimum zone (OMZ), with O_2 concentrations of below ~50 µM extending down to Site U1341 in ~2200 m water depth (Roden, 1995; Takahashi et al., 2011). Although depth and intensity of the OMZ likely changed with time, finely laminated sediment intervals (Takahashi et al., 2011) and trace metal contents (Wehrmann et al., 2013) document suboxic to anoxic sea floor conditions at Site U1341 for most of the last 4 Ma, most likely leading to Fe-bound and organic P release from the sediments.

Upon further sediment burial, the remaining Fe-bound and organic P as well as fish remains are transformed into stable, well-crystallised CFA via sink switching (Ruttenberg, 2001; Paytan and Faul, 2007). At Site U1341, the pore water profiles of iron, alkalinity and phosphate point to most intense organic matter remineralisation in the upper ~30 m of the sediment section (Takahashi et al., 2011). Below this depth, phosphate concentrations decrease from ~50 µM along a "concave-down" profile to ~10 µM below ~300 m sediment depth, similar to pore water phosphate profiles in the Sea of Japan (Föllmi and Von Breymann, 1992). This pore water profile documents that sink switching and disperse CFA formation below ~30 m sediment depth (at the expense of organic and Fe-bound P) is and was taking place at Site

U1341 (Fig. 8) (Ruttenberg and Berner, 1993; Filippelli and Delaney, 1996; Delaney, 1998; Anderson et al., 2001). At the same time, sink switching and redox-controlled P release to the water column effectively limit our ability to reconstruct the original accumulation rates of Fe-bound and organic P at Site U1341. Also the overall low TOC values - which stand in contrast to the high biogenic opal contents – indicate that significant early diagenesis has overprinted the original TOC record, as shown by Wehrmann et al. (2013).

4.1.3 The dominance and variability of carbonate fluorapatite: Authigenic versus detrital

As described above, sink switching is considered to be the dominant process that leads to the formation of CFA in ocean sediments worldwide, and to the long-term burial of P in marine deposits (e.g., Froelich et al., 1982, 1983; Ruttenberg and Berner, 1993; Föllmi, 1996; Filippelli, 2008). As this process starts within the first few meters of the sediment column (e.g., Faul and Delaney, 2000; Küster-Heins et al., 2010a, b), the CFA contribution to the total P pool usually increases with progressive sediment burial (e.g., Filippelli and Delaney, 1996; Delaney, 1998; Anderson et al., 2001). This trend is also observed at Site U1341 (Fig. 4). However, there is another pattern superimposed on the CFA record that is evident from comparison with the Al record; the highest contents of CFA consistently occur in Al-rich (detrital) intervals while they are lower in the Si_{xs}-rich (biosiliceous) layers (Figs. 4, 5a). This positive Al-CFA relationship either indicates that authigenic CFA preferential formed within the fine-grained terrigenous sediment layers, or that CFA was delivered together with terrigenous material from continental sources (by wind, rivers, or sea ice). The latter explanation is favoured for several reasons: (a) If CFA formed within the Al-rich

layers due to sink switching, the labile precursor phases (Fe-bound P, organic P, fish remains) must have been enriched in the Al-rich layers as well. However, both organic P and fish remains were likely enriched within the biosilica-rich sediment layers that formed due to increased productivity and export of biogenic material to the sea floor, leaving only Fe-bound P as a labile P fraction potentially enriched in the Al-rich sediment layers. (b) There is no significant correlation between Al and TOC contents at Site U1341 (Fig. 2; $R^2 = 0.16$, not shown) that would indicate a coupling of organic matter to clay mineral surfaces. (c) Even if significant amounts of organic matter were exported to the sea floor in association with fine-grained Al-rich detritus, this organic matter would have been more refractory than the fresh algal material deposited within the biosilica-rich layers, and thus less likely to release organic P compounds. (d) Authigenic phases like CFA usually precipitate where sedimentary pore space is available, and biosiliceous deposits have higher porosities than clay-rich terrigenous layers. We therefore conclude that the clear positive correlation of CFA with Al at Site U1341 is due to a significant terrigenous contribution to the CFA record. The idea of terrigenous CFA input into the ocean is not new, and is discussed in several studies from different depositional and climatic regimes worldwide (Fig. 9, numbers 1-18), allowing the Bering Sea to be considered within a global perspective.

With respect to riverine CFA input, Berner and Rao (1994) found that CFA makes up 16-30% of total P in suspended and bank sediments of the Amazon River, while it was 5-7% of total P in Lagunitas Creek (~40 km north of San Francisco, California) (Vink et al., 1997). Compton et al. (1993, 2002) found that most CFA grains in shelf deposits off Florida and South Africa were reworked from older phosphorites. While no studies exist for the rivers discharging into the Bering Sea, Zhang et al. (2010)

found a CFA contribution of ~13% of total P on the Bering Sea shelf, most probably related to the weathering and erosion of CFA-rich sedimentary rocks in the Alaskan hinterland (Patton and Matzko, 1959; Mull et al., 1982; Parrish et al., 2001). This river/shelf-derived CFA could have been transported to Bowers Ridge as suspension load by currents or sea ice (Fig. 8) (Van Laningham et al., 2009).

Regarding potential eolian input of CFA to the North Pacific, Flaum (2008) and Guo et al. (2011) found that in sediments of the Chinese Loess Plateau and Inner Mongolia, 40-74% of total P occurs as CFA. Dust from these Asian regions is deposited over the North Pacific (including the Bering Sea), so eolian deposition may not only have contributed significantly to the CFA budget at Site U1341, but also to the wider ocean region (Fig. 9) (Nakai et al., 1993; Rea, 1994; Mahowald et al., 2011). The dominance of CFA in eolian and riverine sediment, and its imprint on the P speciation of marine sediments, has also been described for the Mediterranean (Eijsink et al., 2000), the Red Sea (Anderson et al., 2010), the Gulf of California and Santa Barbara Basin (Lyons et al., 2011; Sekula-Wood et al., 2012), and the Arabian Sea (Kraal et al., 2012).

In conclusion, a significant portion of CFA at Site U1341 appears to be terrigenous despite the open marine location of Bowers Ridge, and this seems to be true for marine deposits from other climatic and depositional settings as well (Föllmi, 1996 and references therein; Compton et al., 2000; Föllmi et al., 2005; Kraal et al., 2012). Our study adds fully marine high-latitude environments to this list, providing they receive appreciable amounts of terrigenous material by wind, sea ice, or currents. Implications for the general interpretation of marine P records are significant (Fig. 9), especially for the question of how much of the operationally defined reactive P was readily bioavailable at the time of deposition.

Following the approach of Ruttenberg (2003), we estimate the average contribution of detrital CFA at Site U1341 by assuming that the *in situ* formation of authigenic CFA should be lowest directly below the sediment-water interface, and that the detrital CFA input was invariable through time. Although the shallowest sample at Site U1341 was taken significantly below the sediment-water interface (4.4 m CCSF-B), its CFA contribution to total P (23.8%) is close to the minimum analysed value (17.8% at 22.7 m CCSF-B), and is thus considered the average contribution of detrital CFA at Site U1341. When comparing this value with the average contribution of CFA to total P over the whole record (~35%), around 2/3 of the buried CFA at Site U1341 would be of detrital origin. Taking the lowest CFA content of 17.8% as the average detrital CFA background at Site U1341, the detrital contribution to the CFA record would be on average ~50%. This more conservative estimate would still reduce the average reactive P MAR at Site U1341 by ~25%, from 57.5 to 42.7 μmol/cm^2/ka (including opal-bound P) (Fig. 6a).

4.1.4 The significance of opal-bound P in biosiliceous sediments

This study shows that biogenic opal-bound P can be an important sink for reactive P in biosilica-dominated regimes like the Bering Sea and elsewhere (Fig. 9, letters a-e). Latimer et al. (2006) showed that in opal-rich Southern Ocean sediments (Fig. 9), the recognition of opal-bound P significantly increased the reactive P fraction. However, beyond the operational separation of the opal-bound P fraction, the precise nature of this biosilica-P coupling is unclear. At Site U1341, we show for the first time that the highest contents of opal-bound P are directly related to maxima in the Si_{xs} record (i.e., biogenic opal) (Figs. 2, 4, 7), while in the Southern Ocean sediments studied by

Latimer et al. (2006), the relationship between biosilica content and opal-bound P was less clear. The latter was explained by opal diagenesis at the Southern Ocean sites, leading to partial post-depositional release of opal-associated P to the pore waters. While opal-bound P diagenesis likely occurred at Site U1341 as well (see below), the weak opal-P relationships observed by Latimer et al. (2006) might be artefacts of the photometric opal-bound P quantification (Strickland and Parsons, 1972) that also posed a challenge at Site U1341 (see Material and Methods section). Given the good Si_{xs} to opal-bound P correlation at Site U1341 (Fig. 7), we are confident that ICP-OES analysis of the opal-bound P fraction yields more reliable data.

Based on the correlation of opal-bound P with the Si_{xs} record, it can be assumed that the opal-bound P record indeed documents a primary depositional signal (i.e., the direct incorporation of opal-bound P during biogenic opal formation). There are several possible explanations for this biosilica-P coupling: (a) Phosphorus incorporated into biosiliceous diatom frustules as highly phosphorylated proteins (silaffins, silacidins), which play a critical role in biosilica morphogenesis (Kröger et al., 2002; Poulsen et al., 2003; Sumper and Kröger, 2004; Sumper and Brunner, 2008; Wenzl et al., 2008; Richthammer et al., 2011). Biosilica-bound P was also found in soil phytoliths (Giguet-Covex et al., 2013), supporting a tight biosilica-P coupling in the natural environment; (b) Phosphorus stored within diatom cells as polyphosphate, which has been suggested as a major component of P cycling in diatom-dominated aquatic systems (Diaz et al., 2008; Nunez-Milland et al., 2010; Orchard et al., 2010; Diaz et al., 2012). (c) Organic matter-bound P protected within the diatom frustules during organic P extraction and released upon frustule dissolution (Latimer et al., 2006; Abramson et al., 2009). Option (b) is unlikely

because polyphosphate is originally associated with the organic tissue of the diatom cells and seems to be quickly released during diagenesis, potentially contributing to CFA precipitation (Diaz et al., 2008, 2012). Therefore, any polyphosphate-sourced P would have been released during steps 3 or 5 of the sequential extraction. Option (c) is unlikely because the protection of organic P within intact diatom frustules would be a function of frustule preservation at the sea floor (e.g., Ragueneau et al., 2000), which at Site U1341 was lowest in the interval with highest opal-associated P (Aiello and Ravelo, 2012). It therefore appears that opal-bound P as a structural component of the diatom frustules is the most likely explanation for the biosilica-P coupling at Site U1341. To our knowledge, Si/P ratios of organic-lean opal frustules (i.e., diatom or radiolarian cell walls without organic coating) have rarely been determined directly. The molar Si_{xs}/opal-bound P ratios at Site U1341 (on average 4,730 mol/mol) are orders of magnitude higher than Si/P ratios of modern whole diatom cells under various environmental conditions (1-4 mol/mol after Tesson et al., 2009; 10-120 mol/mol after Baines et al., 2010). However, a diatom frustule cleaned with boiling H_2O_2 (Tesson et al., 2009) had a molar Si/P ratio of ~46, which is close to the lowest Si_{xs}/opal-bound P ratio of ~90 at Site U1341 (Fig. 6b), providing some confidence that opal-bound P at Site U1341 is indeed a structural component of diatom frustules.

Irrespective of the original incorporation process(es), the P-biosilica association appears to be at least partly preserved in the sediments at Site U1341, as indicated by the positive correlation between both parameters. However, the Si_{xs}/opal-bound P ratio shows a clear down-core trend to higher values, ranging from minima < 500 in the uppermost ~40 m CCSF-B, to a maximum of ~10,000 in the lowest sample (Fig. 6b). In detail, the Si_{xs}/opal-bound P ratio correlates positively with sediment age (R^2 = 0.56) and depth (R^2 = 0.56), and even better with Si_{xs} contents (R^2 = 0.76) (Fig. 7).

There are several possible explanations for these co-variations. The original opal-bound P may be released with increasing sediment age and/or burial depth due to diagenetic processes and/or opal re-crystallisation (similar to opal-bound amino acids; King, 1974; Ingalls et al., 2003), and contribute to authigenic CFA formation. Alternatively, variable sedimentary Si_{xs}/opal-bound P ratios could reflect differences in Si-P uptake stoichiometry over time in response to changing environmental conditions, e.g., variable availability of P or micronutrients, or changes in the diatom assemblages (Baines et al., 2010, 2011). Irrespective of the specific Si-P interactions in the water and/or sediment column, our data show that a significant fraction of the opal-bound P pool remains stable under early diagenetic conditions, and contributes to the long-term burial of reactive P in marine sediments. At Site U1341, the inclusion of this opal-bound P fraction into the reactive P budget increases the average reactive P MAR by ~25%, from 43.9 to 57.5 μmol/cm^2/ka (assuming only authigenic CFA) (Fig. 6a).

4.1.5 Terrigenous CFA, opal-bound P, and the marine reactive P budget

We have shown that at IODP Site U1341, a close relationship exists between the CFA-bound P fraction and the detrital sediment input. There also seems to be a strong contribution of opal-bound P to the total P pool that is directly coupled to biogenic opal deposition. The association of these two P fractions with the detrital and biosiliceous components of the sediment, respectively, has a significant impact on the calculation of reactive P MARs in the central Bering Sea, and may have important implications for our understanding of the marine P cycle as a whole (Fig. 8). Findings based on only one sediment record from the Bering Sea cannot be directly

extrapolated to the global ocean, and thus further studies are required to fully consider implications for the global P cycle. Nevertheless, our results agree with other studies from various climatic and depositional environments worldwide (Fig. 9), allowing for an initial consideration of some potential implications for the global marine P cycle.

Comparing reactive P MARs at Site U1341 with published values from other parts of the world ocean supports the view of Bowers Ridge as an open ocean depositional setting, as already suggested by the generally low Al_2O_3 and high Si_{xs} contents (Fig. 2). Irrespective of the inclusion of opal-bound P into, and exclusion of detrital CFA from, the reactive P budget, average reactive P MARs at Site U1341 are between 42.7 and 57.5 $\mu mol/cm^2/ka$, with most samples ranging between 20 and 100 $\mu mol/cm^2/ka$ (Fig. 6a). These reactive P MARs are similar to values from the Equatorial Pacific (Filippelli and Delaney, 1994; Filippelli, 1997), the South China Sea and Sea of Japan (Tamburini and Föllmi, 2009), but 1-2 orders of magnitude lower than values from modern upwelling areas (Arabian Sea, Peru margin; Filippelli and Delaney, 1992; Schenau and de Lange, 2001; Tamburini and Föllmi, 2009). Comparing our data with Latimer et al. (2006), we find that reactive P MARs at Bowers Ridge are on average 4-5 times higher than in the Southern Ocean (ODP Sites 1089 and 1095), but the inclusion of opal-bound P increases reactive P MARs by on average ~25% in both environments. This provides support for the suggestion by Latimer et al. (2006) that in opal-dominated ocean regions, reactive P burial rates might be substantially underestimated. On the other hand, Figure 9 illustrates that many coastal upwelling areas (e.g., off California, Namibia, Morocco, the Arabian Sea), but also open ocean environments (Equatorial Atlantic, North Pacific) may receive significant amounts of detrital CFA via rivers and/or dust, and reactive P

MARs in those areas might have been overestimated. These issues are discussed below in more detail.

Estimates of the oceanic P residence time (Ruttenberg, 1993; Wallmann, 2003; Tamburini and Föllmi, 2009; Wallmann, 2010) usually assume that the CFA fraction extracted during Step 3 represents an authigenic (i.e., reactive) mineral phase, formed by *in situ* sink switching from labile P phases that directly sampled the dissolved marine phosphate reservoir. However, CFA eroded from sedimentary rocks on land would not dissolve under normal marine pH and temperature conditions (Fig. 8) (Guidry and Mackenzie, 2003; Carbo et al., 2005; Harouiya et al., 2007; Anderson et al., 2010; Furutani et al., 2010; Savenko, 2010), and should therefore be treated as non-reactive. Defining the CFA fraction as being exclusively derived from the reactive P pool would lead to an overestimation of reactive P burial rates (Compton et al., 2000; Ruttenberg, 2003; Kraal et al., 2012).

As illustrated in Figure 9, detrital CFA input appears to be highest in regions that receive detritus from CFA-rich lithologies (e.g., from the Asian, North African and Arabian deserts, the Inner Asian loess areas, or from black shales) (Eijsink et al., 2000; Chernoff and Orris, 2002; Orris and Chernoff, 2002; Flaum, 2008; Anderson et al., 2010; Furutani et al., 2010; Guo et al., 2011; Kraal et al. 2012). According to Shemesh (1990), these CFA-containing lithologies should be Mesozoic-Cenozoic in age, as in older sedimentary rocks the authigenic CFA is usually recrystallized to carbonate-free fluorapatite, which would be extracted as detrital apatite *sensu* Ruttenberg (1992). Figure 9 also shows that highest terrestrial CFA contents in marine sediments were reported from permanently arid and/or cold regions with dominantly physical weathering (e.g., deserts or polar latitudes) (Eijsink et al., 2000; Flaum, 2008; Anderson et al., 2010; Furutani et al., 2010; Zhang et al., 2010; Kraal

et al., 2012). This seems logical, as prolonged chemical weathering under humid conditions creates acidic soils (e.g., peat bogs, tropical soils), leading to partial dissolution of CFA in the terrestrial environment (Walker and Syers, 1976; Smeck, 1985; Guidry and Mackenzie, 2000, 2003; Le Roux et al., 2006; Harouiya et al., 2007). In open marine regions beyond the immediate influence of river-borne CFA, the deposition of eolian CFA certainly plays a significant role, especially within the Northern Hemisphere "dust belt" between ~10 and ~60°N (Prospero et al., 2002; Maher et al., 2010). In this region, large amounts of potentially CFA-rich dust are redistributed from the Asian, Northern African and Arabian deserts across the North Pacific, Equatorial Atlantic and Arabian Sea, respectively (Fig. 9) (Mahowald et al., 2008; Maher et al., 2010).

Apart from the spatial component in detrital CFA input to the modern ocean, a temporal component can be expected as well for a number of reasons. For example, during glacial periods, arid conditions were globally more widespread than today, resulting in higher dust fluxes across most ocean basins (Rea, 1994; Kohfeld and Harrison, 2001; Latimer and Filippelli, 2001). It can be assumed that more eolian CFA was delivered to the oceans as well, which could have contributed to the high glacial reactive P MARs observed by Tamburini and Föllmi (2009) in glacial sediments underlying the Northern Hemisphere "dust belt" (South China Sea, Sea of Japan, Oman margin, Equatorial Atlantic) (Fig. 9). On the other hand, the potential for detrital CFA transport especially to continental margin sediments was likely higher during de-glacial phases; the melting of continental ice sheets caused increased global river runoff and suspended sediment delivery (including eroded CFA) to the coastal ocean (Marshall and Clarke, 1999; Clark et al., 2001; Menot et al., 2006), while the flooding of continental shelves mobilised and re-deposited pre-

formed CFA in deeper marine settings (Compton et al., 2000; Filippelli et al., 2007). We conclude that detrital CFA input to various marine environments is likely a significant issue on glacial-interglacial timescales, but current extraction methods do not allow a distinction between the detrital and authigenic CFA fractions.

While detrital CFA in marine sediments might lead to an overestimation of marine reactive P burial, excluding opal-bound P from the reactive P budget will have the opposite effect. Our Site U1341 data imply that the amount of opal deposited and preserved at the sea floor has a direct impact on the removal of bioavailable P from the overlying water column, although the exact opal-P binding mechanism remains unclear (Fig. 8). This hypothesis was first established by Latimer et al. (2006) for the Southern Ocean, and their preliminary calculations resulted in shorter oceanic P residence times due to increased reactive P burial in the Southern Ocean. The same should generally apply to other marine settings dominated by biosiliceous productivity (i.e., the North and Equatorial Pacific, and upwelling areas such as off California, Peru/Chile, Namibia, Arabian Sea; Lisitzin, 1996; Hüneke and Henrich, 2011) (Fig. 9).

However, quantifying the opal-bound P sink term is complicated by the shifting extent and geographical location of biosilica deposition with geological time (e.g., Cortese et al., 2004). During interglacials, for example, biosilica accumulation rates were higher than during glacials in many parts of the world ocean (Kohfeld et al., 2005 and references therein), and were most probably accompanied by an increased burial of opal-associated P. On longer time scales, the Eocene was an epoch of increased marine biosilica deposition worldwide (McGowran, 1989; Muttoni and Kent, 2007; Moore, 2008; Stickley et al., 2008), and reactive P burial in direct association with biosilica may have played a significant role in global nutrient

dynamics during past climate conditions. Our understanding of opal-bound P (e.g., occurrence, taxonomic effects, diagenetic stability) is currently too limited to quantify its contribution to global reactive P burial in marine sediments, and further studies in this direction are clearly needed. However, it is evident from this and other studies that biosilica-rich sediments may contain large amounts of reactive P bound within opal frustules, and this potentially significant reactive P sink needs to be accounted for in future research.

5.1 Conclusions and Outlook

Our study shows that in the Bering Sea, but also in comparable modern and paleo-environments (i.e., open marine locations, high biosilica productivity, appreciable terrestrial input by wind/rivers/currents), a revised approach needs to be adopted for a correct interpretation of sedimentary P records. Methodological modifications may lead to a more complete understanding of reactive P burial over wide areas of the global ocean, and hence of marine P dynamics. As the SEDEX scheme often does not extract all sedimentary P, we recommend to determine the total P content independently (i.e., by XRF or ICP-OES analysis) (Ruttenberg, 1992). This will lead to a more realistic estimation of the reactive P contribution to the total P content. In order to recognize potential correlations between the authigenic CFA fraction and the terrigenous sediment component, the SEDEX scheme should be combined with a method that picks up variations in the detrital sediment input (i.e., XRF analysis of detrital elements such as Al and Ti, or mineralogical analyses such as X-ray diffractometry). In combination with more advanced provenance proxies (e.g., Nd-Sr-Pb isotopes) and detailed analyses of the isolated CFA components (e.g., by

electron microscopy), this might ultimately enable us to better distinguish between detrital and truly authigenic CFA. In opal-rich sediments in particular, an additional step should be added to the SEDEX procedure to extract opal-bound P (Latimer et al., 2006). This P fraction may be an important part of the reactive P pool, and its systematic investigation would certainly lead to an improved understanding of the marine P cycle, in particular of the residence times of dissolved phosphate. Further studies of detrital CFA and opal-bound P in marine sediments should cover areas that were and are likely to be affected by these two P fractions (i.e., upwelling areas, the North Pacific, or the Southern Ocean). Despite this spatial aspect, such studies should also be performed on marine deposits representing extreme climate states (e.g., glacial versus interglacial conditions during the Quaternary, or Eocene to Cretaceous greenhouse conditions). Doing so should ultimately lead to a more detailed understanding of the marine P cycle and its interaction with the global climate system.

7.1 References

Abed, A.M., Al Kuisi, M., Khair, H.A., 2009. Characterization of the Khamaseen (spring) dust in Jordan. Atm. Environ. 43, 2868-2876.

Abramson, L., Wirick, S., Lee, C., Jacobsen, C., Brandes, J.A., 2009. The use of soft X-ray spectromicroscopy to investigate the distribution and composition of organic matter in a diatom frustules and a biomimetic analog. Deep-Sea Res. II 56, 1369-1380.

Aiello, I.W., Ravelo, A.C., 2012. Evolution of marine sedimentation in the Bering Sea since the Pliocene. Geosphere 8, 1231-1253.

Algeo, T.J., Ingall, E.D., 2007. Sedimentary C_{org}:P ratios, paleocean ventilation, and Phanerozoic atmospheric pO_2. Palaeogeograph.,Palaeoclimatol., Palaeoecol. 256, 130-155.

Anderson, L.D., Delaney, M.L., Faul, K.L., 2001. Carbon to phosphorus ratios in sediments: implications for nutrient cycling. Global Biogeochem. Cycles 15, 65-79.

Anderson, L.D., Faul, K.L., Paytan, A., 2010. Phosphorus associations in aerosols: what can they tell us about P bioavailability? Mar. Chem. 120, 44-56.

Anschutz, P., Zhong, B., Sundby, B., Mucci, A., Gobeil, C., 1998. Burial efficiency of phosphorus and the geochemistry of iron in continental margin sediments. Limnol. Oceanogr. 43, 53-64.

Baines, S.B., Twining, B.S., Brzezinski, M.A., Nelson, D.M., Fisher, N.S., 2010. Causes and biogeochemical implications of regional differences in silicification of marine diatoms. Glob. Biogeochem. Cyc. 24, GB4031, doi:10.1029/2010GB003856.

Baines, S.B., Twining, B.S., Vogt, S., Balch, W.M., Fisher, N.S., Nelson, D.M., 2011. Elemental composition of equatorial Pacific diatoms exposed to additions of silicic acid and iron. Deep Sea Res. II 58, 512-523.

Bate, D.B., Barrett, J.E., Poage, M.A., Virginia, R.A., 2008. Soil phosphorus cycling in an Antarctic polar desert. Geoderma 144, 21-31.

Baturin, G.N., 2003. Phosphorus cycle in the ocean. Lith. Min. Res. 38, 101-119.

Benitez-Nelson, C.R., 2000. The biogeochemical cycling of phosphorus in marine systems. Earth-Sci. Rev. 51, 109-135.

Benitez-Nelson, C.R., Madden, L.P.O., Styles, R.M., Thunell, R.C., 2007. Inorganic and organic sinking particulate phosphorus fluxes across the oxic/anoxic water column of Cariaco Basin, Venezuela. Mar. Chem. 105, 90-100.

Berner, R.A.. 1973. Phosphate removal from sea water by adsorption on volcanogenic ferric oxides. Earth Planet. Sci. Lett. 18, 77-86.

Berner, R.A., Rao, J.-L., 1994. Phosphorus in sediments of the Amazon River and estuary: implications for the global flux of phosphorus to the sea. Geochim. Cosmochim. Acta 58, 2333-2339.

Campbell, F.R., Thomas, R.L., 1970. Automated method for determining and removing silica interference in determination of soluble phosphorus in lake and stream waters. Envir. Sci. Technol. 4, 602-604.

Chernoff, C.B., Orris, G.J., 2002. Data set of world phosphate mines, deposits, and occurrences – Part A. Geologic data. USGS Open-File Report 02-156-A, 352 pp.

Clark, P.U., Marshall, S.J., Clarke, G.K.C., Hostetler, S.W, Licciardi, J.M., Teller, J.T., 2001. Freshwater forcing of abrupt climate change during the last deglaciation. Science 293, 283-287.

Codispoti, L.A., 1989. Phosphorus vs. nitrogen limitation in new and export production, in: Berger, W.H., Smetacek, V.S., Wefer, G. (Eds.), Productivity of Oceans: Present and Past (eds.). Wiley, Chichester, pp. 372-394.

Compton, J., Mulabisana, J., McMillan, I.K., 2002. Origin and age of phosphorite from the Last Glacial Maximum to Holocene transgressive succession off the Orange River, South Africa. Mar. Geol. 186, 243-261.

Compton, J., Hodell, D.A., Garrido, J.R., Mallinson, D.J., 1993. Origin and age of phosphorite from the south-central Florida Platform: relation of phosphogenesis to sea-level fluctuations and δ^{13}C excursion. Geochim. Cosmochim. Acta 57, 131-146.

Compton, J., Mallinson, D., Glenn, C.R., Filippelli, G., Föllmi, K., Shields, G., Zanin, Y., 2000. Variations in the global phosphorus cycle, in Glenn, C.R., Trevot-Lucas, L., Lucas, J. (Eds.), Marine Authigenesis: From Global to Microbial, SEPM Spec. Publ. 66, pp. 21-33.

Cortese, G., Gersonde, R., Hillenbrand, C.-D., Kuhn, G., 2004. Opal sedimentation shifts in the World Ocean over the last 15 Myr. Earth Planet. Sci. Lett. 224, 509-527.

Cotner, J.B., Ammerman, J.W., Peele, E.R., Bentzen, E., 1997. Phosphorus-limited bacterioplankton growth in the Sargasso Sea. Aquat. Microb. Ecol. 13, 141-149.

Daessle, L.W., Camacho-Ibar, V.F., Carrquiry, J.D., Ortiz-Hernandez, M.C., 2004. The geochemistry and sources of metals and phosphorus in the recent sediments from the Northern Gulf of California. Cont. Shelf Res. 24, 2093-2106.

Delaney, M.L., 1998. Phosphorus accumulation in marine sediments and the oceanic phosphorus cycle. Glob. Biogeochem. Cycles 12, 563-572.

Diaz, J.M., Ingall, E.D., Benitez-Nelson, C., Paterson, D., de Jonge, M., McNulty, I., Brandes, J.A., 2008. Marine polyphosphate: A key player in geologic phosphorus sequestration. Science 320, 652-655.

Diaz, J.M., Ingall, E.D., Snow, S.D., Benitez-Nelson, C.R., Taillefert, M., Brandes, J.A., 2012. Potential role of inorganic polyphosphate in the cycling of phosphorus within the hypoxic water column of Effingham Inlet, British Columbia. Glob. Biogeochem. Cyc. 26, doi:10.1029/2011GB004226.

Dornblaser, M.M., Striegl, R.G., 2007. Nutrient (N, P) loads and yields at multiple cales and subbasin types in the Yukon River basin, Alaska. J. Geophys. Res. 112, G04S57, doi:10.1029/2006JG000366.

Eijsink, L.M., Krom, M.D., Herut, B., 2000. Speciation and burial flux of phosphorus in the surface sediments of the Eastern Mediterranean. Am. J. Sci. 3000, 483-503.

Einsele, W., 1938. Über chemische und kolloidchemische Vorgänge in Eisenphosphat-Systemen unter limnochemischen und limnogeologischen Gesichtspunkten. Arch. Hydrobiol. 33, 361-387.

Expedition 323 Scientists, 2010. Bering Sea Paleoceanography: Pliocene-Pleistocene paleoceanography and climate history of the Bering Sea. IODP Prel. Rept. 323, doi:10.2204/iodp.pr.323.2010.

Faul, K.L., Paytan, A., Delaney, M.L., 2005. Phosphorus distribution in sinking oceanic particulate matter. Mar. Chem. 97, 307-333.

Filippelli, G.M., 2001. Carbon and phosphorus cycling in anoxic sediments of the Saanich Inlet, British Columbia. Mar. Geol.174, 307-321.

Filippelli, G.M., 2008. The global phosphorus cycle: past, present, and future. Elements 4, 89-95.

Filippelli, G.M., Delaney, M. L., 1992. Similar phosphorus fluxes in ancient phosphorite deposits and a modern phosphogenic environment. Geology 20, 709-712.

Filippelli, G.M., Delaney, M.L., 1994. The oceanic phosphorus cycle and continental weathering during the Neogene. Paleoceanography 9, 643-652.

Filippelli, G.M., Delaney, M.L., 1996. Phosphorus geochemistry of equatorial Pacific sediments.Geochim. Cosmochim. Acta 60, 1479-1495.

Filippelli, G.M., Latimer, J.C., Murray, R.W., Flores, J.-A., 2007. Productivity records from the Southern Ocean and the equatorial Pacific Ocean: Testing the glacial shelf-nutrient hypothsis. Deep-Sea Res. II 54, 2443-2452.

Flaum, J.A., 2008. Investigation of phosphorus cycle dynamics associated with organic carbon burial in modern (North Pacific) and ancient (Devonian and Cretaceous) marine systems; strengths and limitations of sequentially extracted (SEDEX) phosphorus data. Dissertation Thesis, Northwestern University, 196 pp.

Föllmi, K.B.. 1996. The phosphorus cycle, phosphogenesis and marine phosphate-rich deposits. Earth-Sci. Rev. 40, 55-124.

Föllmi, K.B., Von Breymann, M., 1992. Phosphates and glauconites of Sites 798 and 799, in Pisciotto, K.A., Ingle, J.C., Von Breymann, M., Barron, J. (Eds.), Proc. ODP Sci. Results 127/128), Ocean Drilling Program, Texas A&M University, pp. 63-74.

Föllmi, K.B., Badertscher, C., De Kaenel, E., Stille, P., John, C.M., Adatte, T., Steinmann, P., 2005. Phosphogenesis and organic-carbon preservation in the Miocene Moneterey Formation at Naples Beach, California – The Monterey Hypothesis revisited. Geol. Soc. Am. Bull. 117, 589-619.

Froelich, P.N., Bender, M.L., Luedtke, N.A., Heath, G.R., Devries, T., 1982. The marine phosphorus cycle. Am. J. Sci. 282, 474-511.

Froelich, P.N., Kim, K.-H., Jahnke, R.A., Burnett, W.C., Soutar, A., Deakin, M., 1983. Pore water fluoride in Peru continental margin sediments: uptake from seawater. Geochim. Cosmochim. Acta 47, 1605-1612.

Froelich, P.N., Arthur, M.A., Burnett, W.C., Deakin, M., Hensley, V., Jahnke, R.A., Kaul, L., Kim, K.-H., Roe, K., Soutar, A., Vathakanon, C., 1988. Early diagenesis of organic matter in Peru continental margin sediments: phosphorite precipitation. Mar. Geol. 80, 309-343.

Furutani, H., Meguro, A., Iguchi, H., Uematsu, M., 2010. Geographical distribution and sources of phosphorus in atmospheric aerosols over the North Pacific Ocean. Geophys. Res. Lett.37, L03805, doi:10.1029/2009GL041367.

Gächter, R., Meyer, J.S., Mares, A., 1988. Contribution of bacteria to release and fixation of phosphorus in lake sediments. Limnol. Oceanogr. 33, 1542-1558.

Giguet-Covex, C., Poulenard, J., Chalmin, E., Arnaud, F., Rivard, C., Jenny, J.-P., Dorioz, J.-M., 2013. XANES spectroscopy as a tool to trace phosphorus

transformation during soil genesis and mountain ecosystem development from lake sediments. Geochim. Cosmochim. Acta 118, 129-147.

Guidry, M.W., Mackenzie, F.T., 2000. Apatite weathering and the Phanerozoic phosphorus cycle. Geology 28, 631-634.

Guidry, M.W.. Mackenzie, F.T., 2003. Experimental study of igneous and sedimentary apatite dissolution: controls of pH, distance from equilibrium, and temperature on dissolution rates. Geochim. Cosmochim. Acta 67, 2949-2963.

Guo, B., Yang, H., Li, Y., 2011. The speciation of phosphorus in the sand particles in western Inner Mongolia. Proceedings, Second International Conference on Mechanic Automation and Control Engineering (MACE), 2755-2757, doi:10.1109/MACE.2011.5987555.

Gunnars, A., Blomqvist, S., Martinsson, C., 2004. Inorganic formation of apatite in brackish seawater from the Baltic Sea: an experimental approach. Mar. Chem. 91, 15-26.

Harouiya, N., Chairat, C., Köhler, S.J., Gout, R., Oelkers, E.H., 2007. The dissolution kinetics and apparent solubility of natural apatite in closed reactors at temperatures from 5 to 50 °C and pH from 1 to 6. Chem. Geol. 244, 554-568.

He, H., Chen, H., Yao, Q., Qin, Y., Mi, T., Yu, Z., 2009. Behaviour of different phosphorus species in suspended particulate matter in the Changjiang estuary. Chin. J. Oceanol. Limnol. 27, 859-868.

Henriksen, A., 1966. Interference from silica in phosphate analysis. Analyst 91, 290-291.

Hüneke, H,Henrich, R., 2011. Chapter 4 – Pelagic sedimentation in modern and ancient oceans. In Hüneke, H., Mulder, T. (Eds.), Deep-Sea Sediments, Developments in Sedimentology 63, Elsevier, pp. 215-351.

Ingall, E.D., Van Cappellen, P., 1990. Relation between sedimentation rate and burial of organic phosphorus and organic carbon in marine sediments. Geochim. Cosmochim. Acta 54, 373-386.

Ingall, E.D., Jahnke, R.A., 1997. Influence of water column anoxia on the elemental fractionation of carbon and phosphorus during sediment diagenesis. Mar. Geol. 139, 219-229.

Ingall, E.D., Bustin, R.M., Van Cappellen, P., 1993. Influence of water column anoxia on the burial and preservation of carbon and phosphorus in marine shales. Geochim. Cosmochim. Acta 57, 303-316.

Ingalls, A.E., Lee, C., Wakeham, S.G., Hedges, J.I., 2003. The role of biominerals in the sinking flux and preservation of amino acids in the Southern Ocean along 170ºW. Deep-Sea Res. II 50, 713-738.

Jahnke, R.A., Emerson, S.R., Roe, K.V., Burnett, W.C., 1983. The present day formation of apatite in Mexican continental margin sediments. Geochim. Cosmochim. Acta 47, 259-266.

Jilbert, T., Slomp, C.P., Gustafsson, B.G., Boer, W., 2011. Beyond the Fe-P-redox connection: preferential regeneration of phosphorus from organic matter as a key control on Baltic Sea nutrient cycles. Biogeosciences 8, 1699-1720.

Jordan, T.E., Cornwell, J.C., Boynton, W.R., Anderson, J.T., 2008. Changes in phosphorus biogeochemistry along an estuarine salinity gradient: the iron conveyer belt. Limnol. Oceanogr. 53, 172-184.

King, K., 1974. Preserved amoni acids from silicified protein in fossil Radiolaria. Nature 252, 690-692.

Kohfeld, K.E., Harrison, S.P., 2001. DIRTMAP: the geological record of dust. Earth-Sci. Rev. 54, 81-114.

Kohfeld, K.E., Le Quere, C., Harrison, S.P., Anderson, R.F., 2005. Role of marine biology in glacial-interglacial CO_2 cycles. Science 308, 74-78.

Kraal, P., Slomp, C.P., De Lange, G.J., 2010. Sedimentary organic carbon to phosphorus ratios as a redox proxy in Quaternary records from the Mediterranean. Chem. Geol. 277, 167-177.

Kraal, P., Slomp, C.P., Forster, A., Kuypers, M.M.M., Sluijs, A., 2009. Pyrite oxidation during sample storage determines phosphorus fractionation in carbonate-poor anoxic sediments. Geochim. Cosmochim. Acta 73, 3277-3290.

Kraal, P., Slomp, C.P., Reed, D.C., Reichart, G.-J., Poulton, S.W., 2012. Sedimentary phosphorus and iron cycling in and below the oxygen minimum zone of the northern Arabian Sea. Biogeosciences 9, 2609-2623.

Krishnamurthy, A., Moore, J.K., Mahowald, N., Luo, C., Zender, C.S., 2010. Impacts of atmospheric nutrient inputs on marine biogeochemistry. J. Geophys. Res. 115, G01006, doi:10.1029/2009JG001115.

Kröger, N., Lorenz, S., Brunner, E., Sumper, M., 2002. Self-assembly of highly phosphorylated silaffins and their function in biosilica morphogenesis.Science 298, 584-586.

Krom, M.D., Kress, N., Benner, S., Gordon, L.I., 1991. Phosphorus limitation of primary productivity in the eastern Mediterranean Sea. Limnol. Oceanogr. 36, 424-432.

Küster-Heins, K., De Lange, G.J., Zabel, M., 2010a. Benthic phosphorus and iron budgets for three NW African slope sediments: a balance approach. Biogeosciences 7, 469-480.

Küster-Heins, K., Steinmetz, E., De Lange, G.J., Zabel, M., 2010b. Phosphorus cycling in marine sediments from the continental margin off Namibia. Mar. Geol. 274, 95-106.

Lanzetta, P.A., Alvarez, L.J., Reinach, P.S., Candia, O.A., 1979. An improved assay for nanomole amounts of inorganic phosphate. Anal. Biochem. 100, 95-97.

Latimer, J.C., Filippelli, G.M., 2001. Terrigenous input and paleoproductivity in the Southern Ocean.Paleoceanography 16, 627-643.

Latimer, J.C., Filippelli, G.M., Hendy, I., Newkirk, D.R., 2006. Opal-associated particulate phosphorus: implications for the marine P cycle. Geochim. Cosmochim. Acta 70, 3843-3854.

Le Roux, G., Laverret, E., Shotyk, W., 2006. Fate of calcite, apatite and feldspars in an ombrotrophic peat bog, Black Forest, Germany. J. Geol. Soc. 163, 641-646.

Li, Y., Yu, J.-J., 1999. Geochemical characteristics of phosphorus near the Huanghe River estuary. Chin. J. Oceanol. Limnol. 17, 359-365.

Lisitzin, A.P., 1996. Oceanic Sedimentation: Lithology and Geochemistry. AGU, Washington D.C., 400 pp.

Liu, S.M., Zhang, J.. Li, D.J., 2004. Phosphorus cycling in sediments ofthe Bohai and Yellow Seas. Est. Coast. Shelf Sci. 59, 209-218.

Lukkari, K., Hartikainen, H., Leivuori, M., 2007a. Fraction of sediment phosphorus revisited: I. Fractionation steps and their biogeochemical basis. Limnol. Oceanogr. Methods 7, 433-444.

Lukkari, K., Leivuori, M., Hartikainen, H., 2007b. Fraction of sediment phosphorus revisited: II. Changes in phosphorus fractions during sampling and storage in the presence or absence of oxygen. Limnol. Oceanogr. Methods 5, 445-456.

Lyons, G., Benitez-Nelson, C.R., Thunell, R.C., 2011. Phosphorus composition of sinking particles in the Guaymas Basin, Gulf of California. Limnol. Oceanogr. 56, 1093-1105.

März, C., Schnetger, B., Brumsack, H.-J., 2013. Nutrient leakage from the North Pacific to the Bering Sea (IODP Site U1341) following the onset of Northern Hemispheric Glaciation? Paleoceanography 28, 1-11.

März, C., Poulton, S.W., Beckmann, B., Küster, K., Wagner, T., Kasten, S., 2008. Redox sensitivity of P cycling during marine black shale formation: dynamics of sulfidic and anoxic, non-sulfidic bottom waters. Geochim. Cosmochim. Acta 72, 3703-3717.

Maher, B.A., Prospero, J.M., Mackie, D., Gaiero, D., Hesse, P.P., Balkanski, Y. 2010. Global connections between aeolian dust, climate and ocean biogeochemistry at the present day and at the last glacial maximum. Earth Sci. Rev. 99, 61-97.

Mahowald, N., Albani, S., Engelstaedter, S., Winckler, G., Goman, M., 2011. Model insight into glacial-interglacial paleodust records. Quat. Sci. Reviews 30, 832-854.

Mahowald, N., Jickells, T.D., Baker, A.R., Artaxo, P., Benitez-Nelson, C.R., Bergametti, G., Bond, T.C., Chen, Y., Cohen, D.D., Herut, B., Kubilay, N., Losno, R., Luo, C., Maenhaut, W., McGee, K.A., Okin, G.S., SiefertR.L., Tsukuda, S. 2008. Global distribution of atmospheric phosphorus sources, concentrations and deposition rates, and anthropogenic impacts. Global Biogeochem. Cycles 22, GB4026, doi:10.1019/2008GB003240.

Malek, M.A., Kim, B., Jung, H.-J., Song, Y.-C., Ro, C.-U., 2011. Single-particle mineralogy of Chinese soil particles by the combined use of low-z particle electron probe X-ray microanalysis and attenuated total reflectance-FT-IR imaging techniques. Anal. Chem. 83, 7970-7977.

Marshall, S.J., Menot, G.K.C., 1999. Modeling North American freshwater runoff through the last glacial cycle. Quat. Res. 52, 300-315.

Matijevic, S., Kuspilic, G., Kljakovic-Gaspic, Z., Bogner, D., 2008. Impact of fish farming on the distribution of phosphorus in sediments in the middle Adriatic area. Mar. Poll. Bul. 56, 535-548.

McGowran, B., 1989. Silica burp in the Eocene ocean. Geology 17, 857-860.

Menot, G., Bard, E., Rostek, F., Weijers, J.W.H., Hopmans, E.C., Schouten, S., Sinninghe Damste, J.S., 2006. Early reactivation of European rivers during the last deglaciation. Science 313, 1623-1625.

Moore, T.C., 2008. Chert in the Pacific: biogenic silica and hydrothermal circulation. Palaeogeogr., Palaeoclimat., Palaeoecol. 261, 87-99.

Moreno, T., Querol, X., Castillo, S., Alastuey, A., Cuevas, E., Herrmann, M., Mounkaila, M., Elvira, J., Gibbons, W., 2006. Geochemical variations in aeolian mineral particles from the Sahara-Sahel dust corridor. Chemosphere 65, 261-270.

Mort, H.P., Slomp, C.P., Gustafsson, B.G., Andersen, T.J., 2010. Phosphorus recycling and burial in Baltic Sea sediments with contrasting redox conditions. Geochim. Cosmochim. Acta 74, 1350-1362.

Mull, C.G., Tailleur, I.L., Mayfield, C.F., Ellersieck, I., Curtis, S., 1982. New Upper Paleozoic and Lower Mesozoic stratigraphic units, central and western Brooks Range, Alaska. AAPG Bull. 66, 348-362.

Muttoni, G., Kent, D.V., 2007. Widespread formation of cherts during the early Eocene climate optimum. Palaeogeogr., Palaeoclimat., Palaeoecol. 253, 348-362.

Naka, S., Halliday, A.N., Rea, D.K., 1993. Provenance of dust in the Pacific Ocean. Earth Planet. Sci. Lett. 119, 143-157.

Neal, C., Neal, M., Wickham, H., 2000. Phosphate measurement in natural waters: two examples of analytical problems associated with silica interference using phosphomolybdic acid methodologies. Sci. Total Environ. 251/252, 511-522.

Nilsen, E.B., Delaney, M.L., 2005. Factors influencing the biogeochemistry of sedimentary carbon and phosphorus in the Sacramento-San Joaquin delta. Estuaries 28, 653-663.

Nunez-Milland, D.R., Baines, S.B., Vogt, S., Twining, B.S., 2010. Quantification of phosphorus in single cells using synchrotron X-ray fluorescence. J. Synchrotron Rad. 17, 560-566.

Onodera, J., Takahashi, K., Nagatomo, R., 2013. Diatoms, silicoflagellates, and ebridians at Site U1341 on the western slope of Bowers Ridge, IODP Expedition 323. Deep-Sea Res. II.

Orchard, E.D., Benitez-Nelson, C.R., Pellechia, P.J., Lomas, M.W., Dyhrman S.T., 2010. Polyphosphate in Trichodesmium from the low-phosphorus Sargasso Sea. Limnol. Oceanogr. 55, 2161-2169.

Orris, G.J., Chernoff, C.B., 2002. Data set of world phosphate mines, deposits, and occurrences – Part B. Location and mineral economic data. USGS Open-File Report 02-156-B, 328 pp.

Parrish, J.T., Droser, M.L., Bottjer, D.J., 2001. A Triassic upwelling zone: the Sublik Formation, Arctic Alaska, U.S.A. J. Sed. Res. 71, 272-285.

Patton, W.W., Matzko, J.J., 1959. Phosphate deposits in northern Alaska. USGS Prof. Paper 302-A, 17 pp.

Paytan, A., Faul, K.L., 2007. The oceanic phosphorus cycle. Chem. Rev. 107, 563-576.

Paytan, A., Cade-Menum, B.J., McLaughlin, K., Faul, K.L., 2003. Selective phosphorus regeneration of sinking marine particles: evidence from ^{31}P-NMR. Mar. Chem. 82, 55-70.

Posner, A.S., Blumenthal, N.C., Betts, F., 1984. The chemistry and structure of precipitated hydroxyapatites, in Nriagu, J.O., Moore, P.B. (Eds), Phosphate Minerals, Springer, pp. 330-350.

Poulsen, N., Sumper, M., Kröger, N., 2003. Biosilica formation in diatoms: Characterization of native Silaffin-2 and its role in silica morphogenesis. PNAS 100, 12075-12080.

Poulton, S.W., Canfield, D.E., 2006. Co-diagenesis of iron and phosphorus in hydrothermal sediments from the southern East Pacific Rise: implications for the evolution of paleoseawater phosphate concentrations. Geochim. Cosmochim. Acta 70, 5883-5898.

Prospero, J.M., Ginoux, P., Torres, O., Nicholson, S.E., Gill, T.E., 2002. Environmental characterization of global sources of atmospheric soil dust identified with the Nimbus 7 Total Ozone Mapping Spectrometer (TOMS) absorbing aerosol product. Rev. Geophys. 40, 1002, doi:10.1029/2000RG000095.

Ragueneau, O., Treguer, P., Leynaert, A., Anderson, R.F., Brzezinski, M.A., DeMaster, D.J., Dugdale, R.C., Dymond, J., Fischer, G., Francois, R., Heinze, C., Maier-Reimer, E., Martin-Jezequel, V., Nelson, D.M., Queguiner, B., 2000. A review of the Si cycle in the modern ocean: recent progress and missing gaps in the application of biogenic opal as a paleoproductivity proxy. Global Planet. Change 26, 317-365.

Rao, L.-J., Berner, R.A., 1997. Time variations of phosphorus and sources of sediments beneath the Chang Jiang (Yangtze River). Mar. Geol. 139, 95-108.

Rea, D.K., 1994. The paleoclimatic record provided by eolian deposition in the deep sea: the geologic history of wind. Rev. Geophys. 32, 159-195.

Richthammer, P., Börmel, M., Brunner, E., Van Pee, K.-H., 2011. Biomineralisation in diatoms: the role of silacidins. ChemBioChem. 12, 1362-1366.

Roden, G.I., 1995. Aleutian Basin of the Bering Sea: thermohaline, oxygen, nutrient, and current structure in July 1993. J. Geophys. Res. 100, 13539-13554.

Ruttenberg, K.C., 1992. Development of a sequential extraction method for different forms of phosphorus in marine sediments. Limnol. Oceanogr. 37, 1460-1482.

Ruttenberg, K.C., 1993. Reassessment of the oceanic residence time of phosphorus.Chem. Geol. 107, 405-409.

Ruttenberg, K.C., 2001. Phosphorus cycle, in:Thorpe, S.A., Turekian, K.K. (Eds.), Encyclopedia of Ocean Sciences 1st Edition. Elsevier, pp. 2149-2162.

Ruttenberg, K.C., 2003. The Global Phosphorus Cycle, in: Holland H.D., Turekian, K.K. (Eds.), Treatise on Geochemistry 8, Elsevier, pp. 585-643.

Ruttenberg, K.C., Berner, R.A., 1993. Authigenic apatite formation and burial in sediments from non-upwelling, continental margin environments. Geochim. Cosmochim. Acta 57, 991-1007.

Ruttenberg, K.C., Ogawa, N.O., Tamburini, F., Briggs, R.A., Colasacco, N.D., Joyce, E., 2009. Improved, high-throughput approach for phosphorus speciation in natural sediments via the SEDEX sequential extraction approach. Limnol. Oceanogr. Methods 7, 319-333.

Savenko, A.V., 2010. On the physicochemical mechanism of diagenetic phosphorite synthesis in the modern ocean. Geochem. Int. 48, 194-201.

Schenau, S.J., De Lange, G.J., 2000. A novel chemical method to quantify fish debris in marine sediments. Limnol. Oceanogr. 45, 963-971.

Schenau, S.J., De Lange, G.J., 2001. Phosphorus regeneration vs. burial in sediments of the Arabian Sea. Mar. Chem. 75, 201-217.

Schenau, S.J., Slomp, C.P., De Lange, G.J., 2000. Phosphogenesis and active phosphorite formation in sediments from the Arabian Sea oxygen minimum zone. Mar. Geol. 169, 1-20.

Sekula-Wood, E., Benitez-Nelson, C.R., Bennett, M.A., Thunell, R., 2012. Magnitude and composition of sinking particulate phosphorus fluxes in Santa Barbara Basin, California. Global Biogeochem. Cycles 26, GB2023, doi:10.1029/2011GB004180.

Shemesh, A., 1990. Crystallinity and diagenesis of sedimentary apatites. Geochim. Cosmochim. Acta 54, 2433-2438.

Slomp, C.P., 2011. Phosphorus cycling in the estuarine and coastal zones: sources, sinks, and transformations, in: Wolanski, E., McLusky, D.S. (Eds.), Treatise on Estuarine and Coastal Science 5. Waltham Academic Press, pp. 201–229.

Slomp, C.P., Van der Gaast, S.J., Van Raaphorst, W., 1996. Phosphorus binding by poorly crystalline iron oxides in North Sea sediments. Mar. Chem. 52, 55-73.

Smeck, N.E., 1985. Phosphorus dynamics in soils and landscapes. Geoderma 36, 185-199.

Steenbergh, A.K., Bodelier, P.L.E., Hoogveld, H.L., Slomp, C.P., Laanbroek, H.J., 2011. Phosphatases relieve carbon limitation of microbial activity in Baltic Sea sediments along a redox gradient. Limnol. Oceanogr. 56, 2018-2026.

Stickley, C.E., Koc, N., Brumsack, H.-J., Jordan, R.W., Suto, I., 2008. A siliceous microfossil view of middle Eocene Arctic paleoenvironments: a window of biosilica production and preservation. Paleoceanography 23, PA1S14, doi:10.1029/2007PA001485.

Strickland, J D.H., Parsons, T.R., 1972. A practical handbook of seawater analysis. Fisheries Research Board of Canada, Ottawa, pp. 45-64.

Suess, E., 1981. Phosphate regeneration from sediments of the Peru continental margin by dissolution of fish debris. Geochim. Cosmochim. Acta 45, 577-588.

Sumper, M., Kröger, N., 2004. Silica formation in diatoms: The function of long-chain polyamines and silaffins. J. Mater. Chem.14, 2059-2065.

Sumper, M., Brunner, E., 2008. Silica biomineralisation in diatoms: the model organism *Thalassiosira pseudonana*. ChemBioChem. 9, 1187-1194.

Sundby, B., Gobeil, C., Silverberg, N., Mucci, A., 1992. The phosphorus cycle in coastal marine sediments. Limnol. Oceanogr. 37, 1129-1145.

Takahashi, K., Ravelo, A.C., Alvarez Zarikian, C., Expedition 323 Scientists, 2011. Proc. IODP 323, Tokyo (Integrated Ocean Drilling Program Management International, Inc.), doi:10.2204/iodp.proc.323.105.2010.

Tallberg, P., Treguer, P., Beucher, C., Corvaisier, R., 2008. Potentially mobile pools of phosphorus and silicon in sediment from the Bay of Brest: interactions and implications for phosphorus dynamics. Est. Coast. Shelf Sci. 76, 85-94.

Tallberg, P., Lukkari, K., Räike, A., Lehtoranta, J., Leivuori, M., 2009. Applicability of a sequential P fractionation procedure to Si in sediment. J. Soils Sed. 9, 594-603.

Tamburini, F., Föllmi, K., 2009. Phosphorus burial in the ocean over glacial-interglacial time scales. Biogeosciences 6, 501-513.

Tesson, B., Masse, S., Laurent, G., Maquet, J., Livage, J., Martin-Jezequel, V., Coradin, T., 2008. Contribution of multi-cellular solid state NMR to the

characterization of the Thalassiosirapseudonana diatom cell wall. Anal. Bioanal. Chem. 390, 1889-1898.

Tesson, B., Genet, M.J., Fernandez, V., Degand, S., Rouxhet, P.G., Martin-Jezequel, V., 2009. Surface chemical composition of diatoms. Chem. Biochem. 10, 2011-2024.

Tyrell, T., 1999. The relative influence of nitrogen to phosphorus on oceanic primary production. Nature 400, 525-531.

Van Cappellen, P., Berner, R.A., 1988. A mathematical model for the early diagenesis of phosphorus and fluoride in marine sediments: apatite precipitation. Am. J. Sci. 288, 289-333.

Van Cappellen, P., Berner, R.A., 1991. Fluorapatite crystal growth from modified seawater solutions. Geochim. Cosmochim. Acta 55, 1219-1234.

Van Cappellen, P., Ingall, E.D., 1996. Redox stabilizations of the atmosphere and oceans by phosphorus-limited marine productivity. Science 271, 493-496.

VanLaningham, S., Pisias, N.G., Duncan, R.A., Clift, P.D., 2009. Glacial-interglacial sediment transport to the Meji Drift, northwest Pacific Ocean: evidence for timing of Beringian outwashing. Earth Planet. Sci. Lett. 277, 64-72.

Vink, S., Chambers, R.M., Smith, S.V., 1997. Distribution of phosphorus in sediments from Tomales Bay, California. Mar. Geol. 139, 157-179.

Virtasalo, J.J., Kohonen, T., Vuorinen, I., Huttula, T., 2005. Sea bottom anoxia in the Archipelago Sea, northern Baltic Sea – implications for phosphorus remineralization at the sediment surface. Mar. Geol. 224, 103-122.

Wallmann, K., 2003. Feedbacks between oceanic redox states and marine productivity: A model perspective focused on benthic phosphorus cycling. Global

Biogeochem. Cycles 17, GB1084, doi:10.1029/2002GB001968.

Wallmann, K., 2010. Phosphorus imbalance in the global ocean? Global Biogeochem. Cycles 24, GB4030, doi:10.1029/2009GB003643.

Walker, T.W., Syers, J.K., 1976. The fate of phosphorus during pedogenesis. Geoderma 15, 1-19.

Wedepohl, K.H., 1995. The composition of the continental crust (Ingerson Lecture). Geochim. Cosmochim. Acta 59, 1217-1232.

Wehrmann, L.M., Arndt, S., März, C., Ferdelman, T.G., Brunner, B., 2013. The evolution of early diagenetic signals in Bering Sea subseafloor sediments in response to varying organic carbon deposition over the last 4.3 Mn. Geochim. Cosmochim. Acta 109, 175-196.

Wenzl, S., Hett, R., Richthammer, P., Sumper, M., 2008. Silacidins: highly acidic phosphopeptides from diatom shells assist in silica precipitation *in vitro*. Angew. Chem. Int. Ed. 47, 1729-1732.

Zhang, J.-Z., Guo, L., Fischer, C.J., 2010. Abundance and chemical speciation of phosphorus in sediments of the Mackenzie River delta, the Chukchi Sea and the Bering Sea: importance of detrital apatite. Aquat. Geochem. 16, 353-371.

8.1 Tables:

Table 1: Extraction scheme according to Ruttenberg (1992), Schenau and De Lange (2000) and Latimer et al. (2006), with extraction procedures, extracted phases, and

relative standard deviations (RSD) determined by triplicate extraction of three representative samples from Site U1341.

9.1 Figures:

Figure 1: Schematic map of the Bering Sea with IODP Site U1341 on Bowers Ridge.

Figure 2: Bulk geochemical profiles of SiO_2, Al_2O_3, Si_{xs}, P_{xs} (determined by XRF) and TOC (shipboard data) (all in wt%) against sediment depth (meters CCSF-B). Excess contents are calculated relative to Upper Continental Crust composition (Wedepohl, 1995), and respective records are displayed as 5-point running means (solid black lines).

Figure 3: Records of P_{xs} (wt%) and extracted P fractions (fish remains, Fe-bound P, carbonate fluorapatite, detrital fluorapatite, organic P, opal-bound P; all in ppm of dry bulk sediment) against sediment depth (meters CCSF-B).

Figure 4: Records of P_{xs} (wt%) and extracted P fractions (fish remains, Fe-bound P, carbonate fluorapatite, detrital fluorapatite, organic P, opal-bound P, residual P; all in relative % of total P) against sediment depth (meters CCSF-B).

Figure 5: (a) Bar chart displaying the relative average contribution of the different extracted P fractions and residual P to total P. (b) Contibutions of reactive P (= sum of all extracted P fractions without detrital P) to total P against sediment depth (meters CCSF-B); values are calculated without opal-bound P, all CFA authigenic (open circles); with opal-bound P, all CFA authigenic (filled circles); with opal-bound P, 50% detrital CFA (squares).

Figure 6: (a) Reactive P MARs (μmol/cm^2/ka) against sediment depth (meters CCSF-B); values are calculated without opal-bound P, all CFA authigenic (open circles); with opal-bound P, all CFA authigenic (filled circles); with opal-bound P, 50% detrital CFA (squares). (c) Molar Si_{xs}/opal-bound P ratios (mol/mol) against sediment depth (meters CCSF-B).

Figure 7: Scatter plots displaying relationships and respective correlation coefficients (R^2) between different geochemical parameters determined by XRF (Si_{xs}, Al), sequential extraction (carbonate fluorapatite, opal-bound P, residual P), combinations of both (Si_{xs}/opal-bound P ratios), and sediment age/depth.

Figure 8: Schematic illustration of the Bering Sea P cycle including input pathways (eolian, riverine); transformation and recycling processes within surface waters, deep/intermediate waters, surface (< 50 m) and deeper (> 50 m) marine sediments; and buried P fractions (after Ruttenberg, 2001; Slomp, 2011 and reference).

Figure 9: Global map displaying terrigenous CFA and opal-bound P sources and sinks. Numbers in squares: Terrestrial carbonate fluorapatite (CFA) detected in loess, dust, river suspension and sediments, marine suspended particles and surface sediments. (1) Kraal et al. (2012); (2) Eijsink et al. (2000); (3) Anderson et al. (2010); (4) Flaum (2008); (5)-(7) Zhang et al. (2010); (8) Berner and Rao (1994); (9) Vink et al. (1997), Nilsen and Delaney (2005), Sekula-Wood et al. (2012); (10) Moreno et al., 2006; (11) Li and Yu (1999), Liu et al. (2004); (12) Daessle et al. (2004); (13) Flaum (2008), Malek et al. (2011); (14) Abed et al. (2009); (15) Bate et al. (2008); (16) Rao and Berner (1997), He et al. (2009); (17) Guo et al. (2011); (18) Lyons et al. (2011). Letters in circles: Opal-associated P extracted from marine sediments. (a)-(c) Latimer et al. (2006); (d) Küster-Heins et al. (2010a); (e) this study). Asterixes:

Phosphorite deposits in high-latitude/arid regions with minimal chemical weathering (Chernoff and Orris, 2002; Orris and Chernoff, 2002). Light gray shading: Major sources of dust to the ocean (Northern Hemisphere "dust belt"; Prospero et al., 2002; Maher et al., 2010). Dark gray shading: Ocean regions potentially receiving CFA-rich dust (Mahowald et al., 2008; Maher et al., 2010). Thick dashed lines: Approximate limits of biogenic opal deposition areas in the modern ocean (Arabian Sea, Southern Ocean, upwelling areas, North Pacific; Lisitzin, 1996; Hüneke and Henrich, 2011).
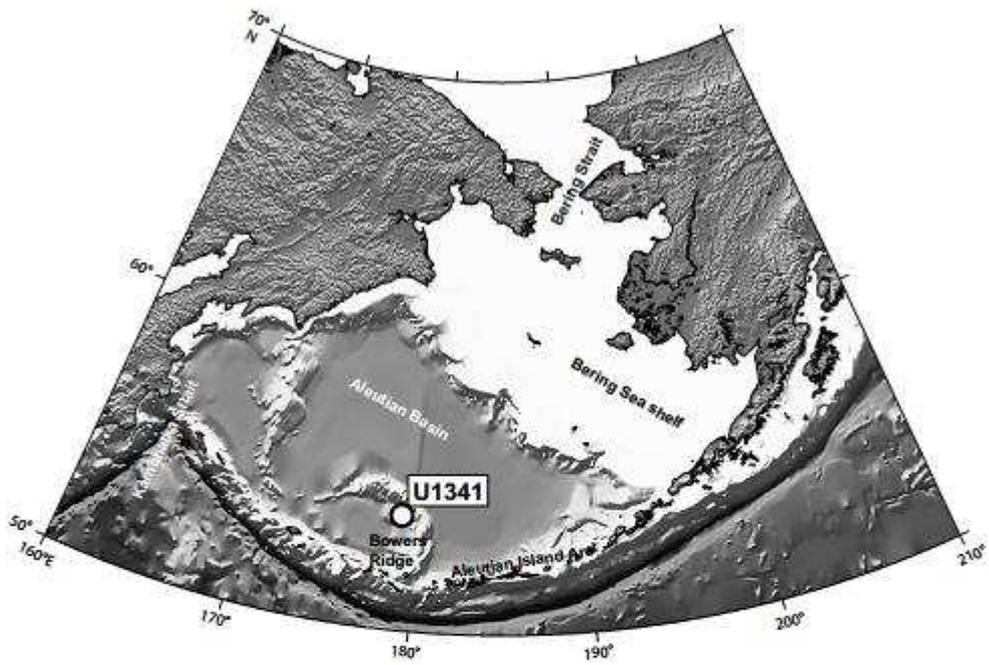
Figure 1
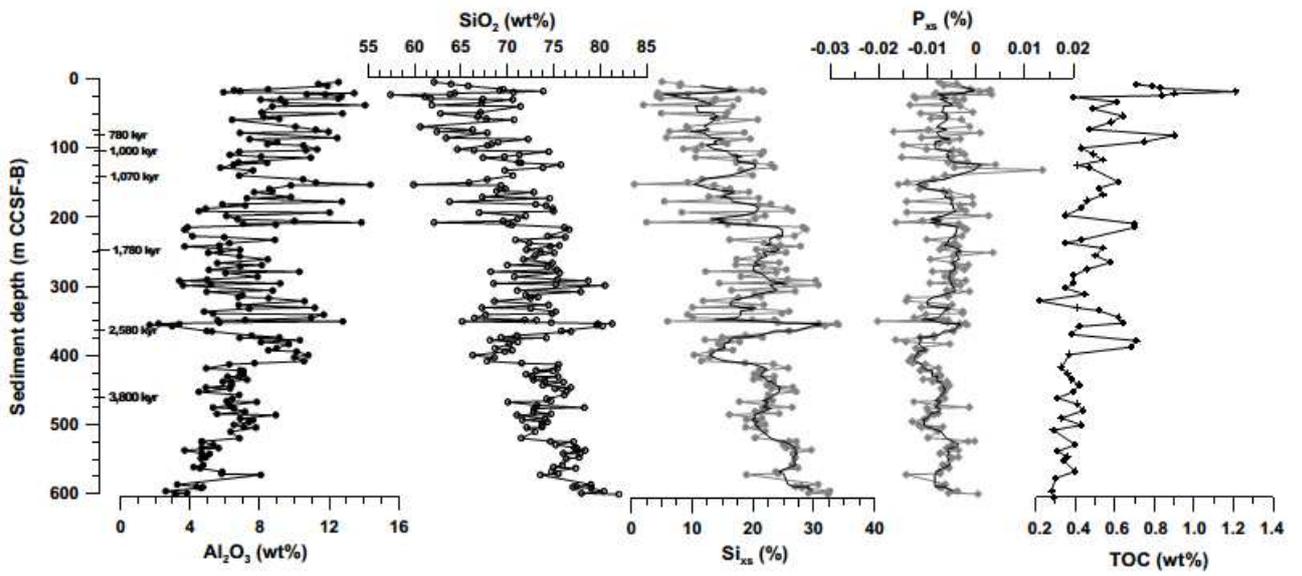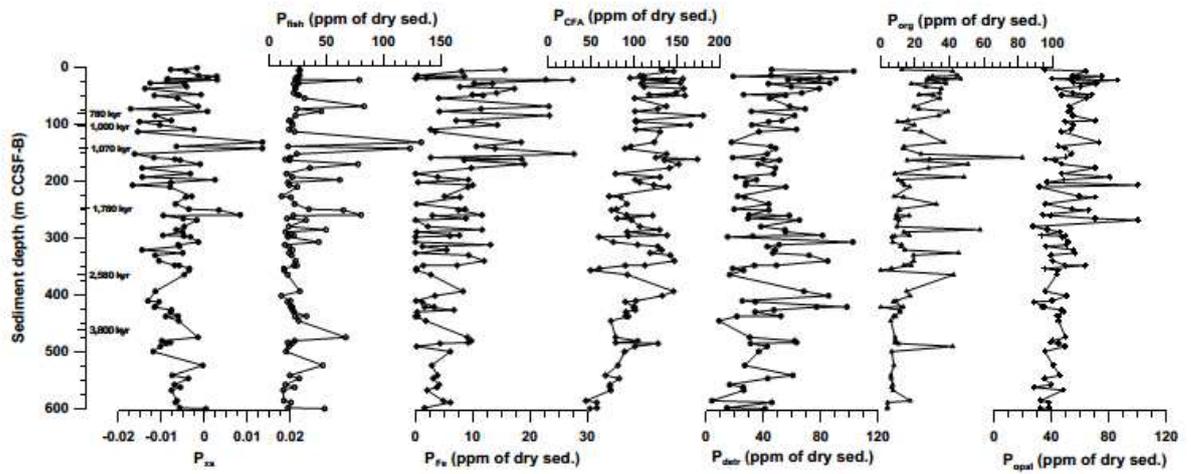
Figure 3
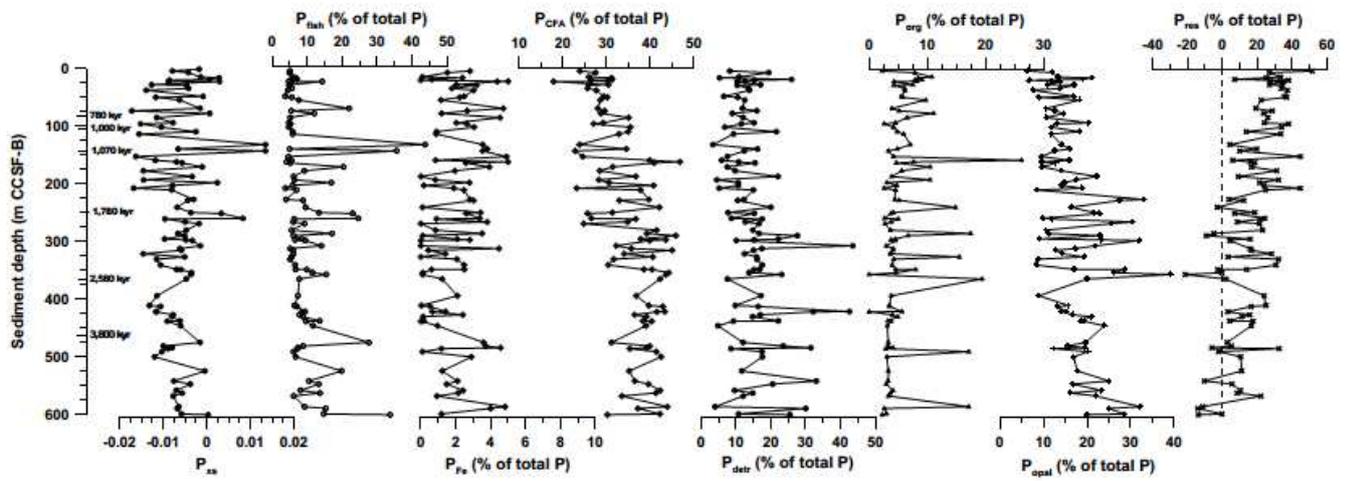
Figure 4
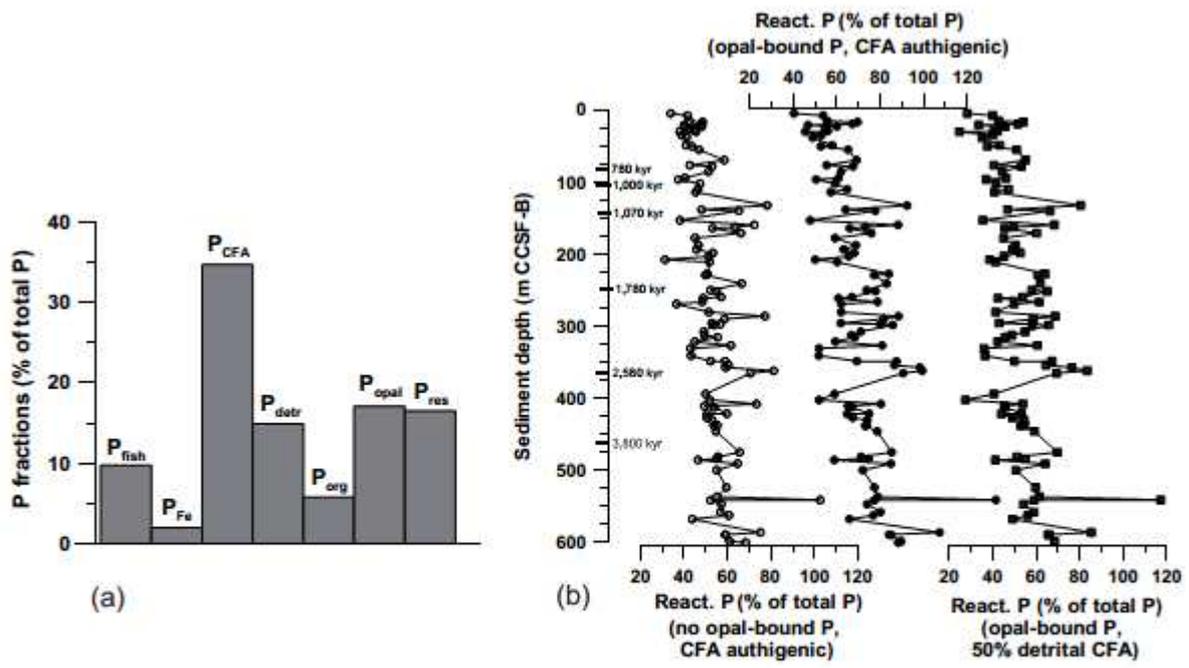
Figure 5
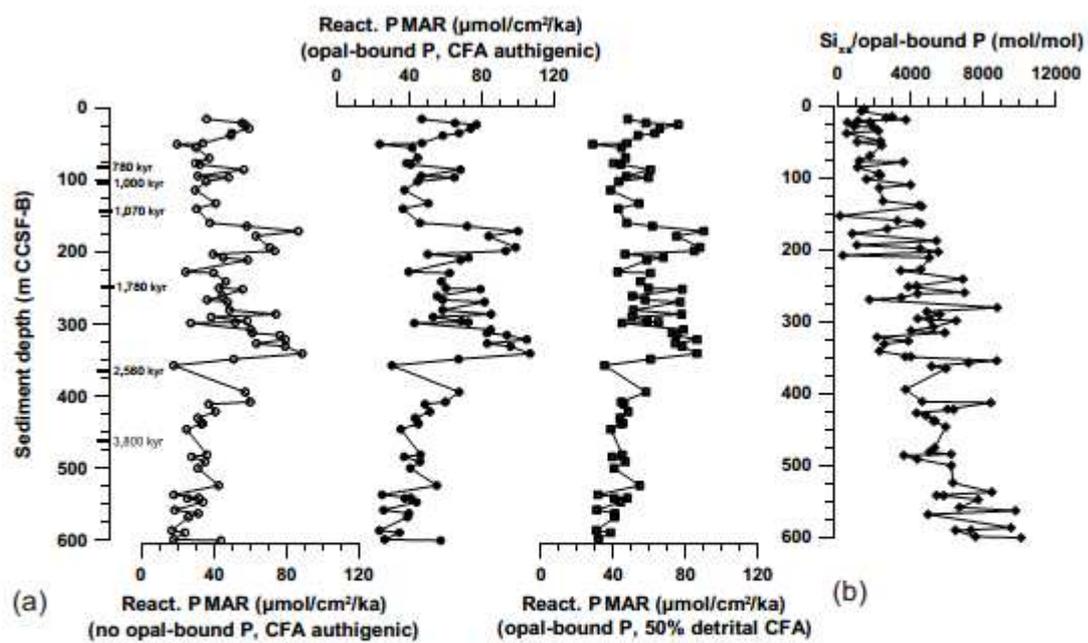
Figure 6
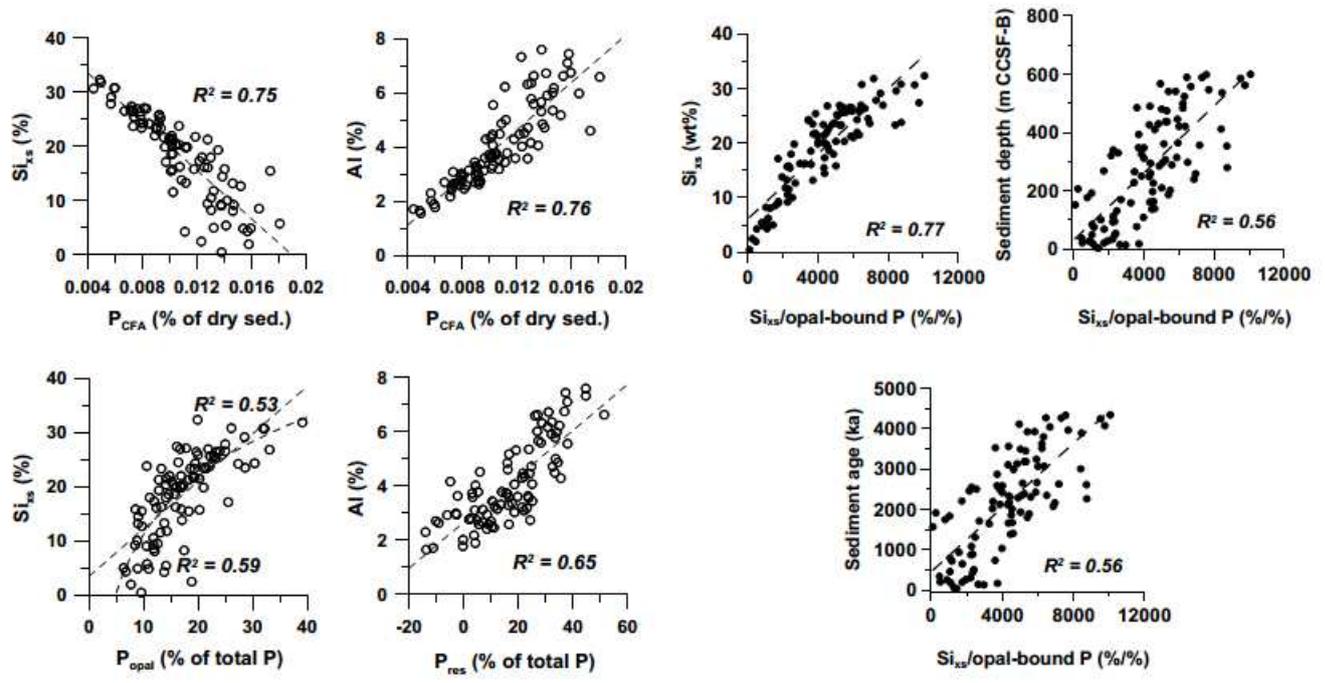
Figure 7

Figure 8

Figure 9